Università degli studi di Napoli Federico II

Scuola di Medicina e Chirurgia

Dipartimento di Scienze Biomediche Avanzate

Direttore Prof. Claudio Buccelli

Dottorato di Ricerca in Scienze Biomorfologiche e Chirurgiche

XXX ciclo

Coordinatore Prof. Alberto Cuocolo

Semi-quantitative evaluation of myocardial perfusion and left ventricular function: comparison between the standard anger and novel CZT camera

Relatore

Prof. Alberto Cuocolo

Candidata

Dott.ssa Valeria Cantoni

Index

Introduction

Single-photon emission computed tomography (SPECT) myocardial perfusion imaging (MPI) is a well-established technique for the diagnosis and risk stratification of patients with suspected or known coronary artery disease (CAD) (1). Conventional Anger camera systems for SPECT imaging use sodium iodide crystals and parallel-hole collimators. However, although the latest developments have enhanced image quality performance of these systems, some technical limits are still present, as poor energy resolution prolonged imaging time, low spatial resolution and the need for relatively large doses of radiopharmaceuticals (2). The novel gamma cameras with semiconductor Cadmium-Zinc-Telluride (CZT) detectors have been introduced recently (2). In this new system, CZT semiconductors, that directly convert radiation into electric signals, have replaced the conventional sodium iodide crystals allowing an improvement in terms of image accuracy and acquisition time (3-5). Different studies demonstrated the good diagnostic performance of these new cameras in the routine clinical practice (2). In particular, previous studies demonstrated that CZT-SPECT provides adequate risk stratification results of patients referred to MPI for their suspected or known CAD (6). Despite a direct comparison between conventional Anger and CZT cameras has been performed (7) in the evaluation of patients referred for MPI, a better correlation of the all semi-quantitative perfusion and functional parameters needs to be provided. Moreover, no studies have been performed using an external validation standard such as coronary angiography for comparing the diagnostic accuracy of the two imaging modalities in the evaluation of patients with suspected or known CAD. Thus, we conducted a retrospective study to compare the ability of CZT camera (D-SPECT) with that of conventional SPECT in detecting myocardial perfusion and functional abnormalities in patients referred for clinical evaluation of suspected or known CAD at our institution using semi-quantitative analysis of myocardial perfusion and function.

Methods

Study Population

Between February 2016 and May 2017, 517 consecutive patients with suspected or known CAD underwent gated stress MPI for the assessment of myocardial ischemia at our institution. Of the 517 patients considered for the purpose of the present investigation, 86 (16%) patients had coronary angiography data available.

Pre-scan likelihood of CAD

As part of the baseline examination, clinical teams collected information on traditional cardiovascular risk factors, including age, gender, blood pressure, smoking history, serum cholesterol, family history of CAD, rest ECG characteristics, diabetes and its complications (including neuropathy, nephropathy, peripheral vascular disease, and retinopathy), as well as the results of ECG stress testing. Hypertension was defined as a known history of systolic blood pressure >140 mmHg or the use of antihypertensive medication. Hypercholesterolemia was defined as a known history of dyslipidemia or treatment with cholesterol-lowering medication. Patients were classified as having diabetes if they had a previous diagnosis of diabetes or were receiving treatment with oral hypoglycemic drugs or insulin. A positive family history of CAD was defined as the presence of CAD in first-degree relatives. These data were verified and complemented with demographic and clinical information collected from medical records. From these clinical variables, the pre-test CAD likelihood was calculated for each patient by dedicated software based on Bayesian analysis of pre-scan patients' data (Cadenza, version 5.04.3, Advanced Heuristics, Inc., Bainbridge Island, Washington) (8). For patients who underwent pharmacologic stress testing, the pre-test likelihood was calculated without using the stress test parameters. . According to pre-test likelihood of CAD, patients with a likelihood score <0.15 were considered at low risk, while those with a score between 0.15 and 0.85 were considered at intermediate risk. In patients with known CAD, the software automatically calculated the pre-test likelihood of ischemia.

Stress protocol

All patients underwent stress technetium-99m (Tc-99m) sestamibi gated MPI by physical exercise or dipyridamole stress test, according to the recommendations of the European Association of Nuclear Medicine and European Society of Cardiology (9). In all patients, beta-blocking medications and calcium antagonists were withheld for 48 hours and long-acting nitrates for 12 hours before testing. For patient undergoing exercise test, symptom-limited treadmill standardized protocols were performed, with monitoring of heart rate and rhythm, blood pressure, and electrocardiography (ECG). Test endpoints were achievement of 85% maximal predicted heart rate, horizontal or downsloping ST-segment depression >2 mm, ST-segment elevation >1 mm, moderate to severe angina, systolic blood pressure decrease >20 mm Hg, blood pressure >230/120 mm Hg, dizziness, or clinically important cardiac arrhythmia. For dipyridamole stress test, patients were instructed not to consume products containing caffeine for 24 hours before the test. Dipyridamole was infused at dose of 0.142 $mg \cdot kg^{-1} \cdot minute^{-1}$intravenous over 4 minutes. A dose of 100 mg of aminophylline was administered intravenously in the event of chest pain or other symptoms, or after significant ST depression. At peak exercise, or 4 minutes after completion of dipyridamole infusion, a bolus of 370 MBq of Tc-99m sestamibi was intravenously injected. Patients continued the exercise for additional 60 seconds after tracer injection. For both types of stress, heart rate, blood pressure, and 12-lead ECG data were recorded at rest, at the end of each stress stage, at peak stress and in the delay phases at rest. Maximal degree of ST-segment change at 80 ms after the J-point of the ECG was measured and assessed as horizontal, downsloping or upsloping. In our institution stress protocol-only is used, thus patients with negative findings were not reinjected at rest.

Conventional SPECT acquisition protocol

Anger camera: E.CAM

For both types of stress, imaging was started 30 minutes after tracer injection using a dual-head rotating gamma camera (E.CAM, Siemens Medical Systems, Hoffman Estates, IL, USA) equipped with a low-energy, high-resolution collimator and connected with a dedicated computer system (10). No attenuation or scatter correction was used. For gating, a cardiac cycle was divided into eight frames. The R-R interval and heart rate histogram were recorded to monitor arrhythmia. An average R-R interval of ±15% was accepted for gating. Perfusion imaging was reconstructed by summing the gated data at each projection into an "ungated" raw data file before low phase prefiltering and ramp filtered back projection. An automated software program (e-soft, 2.5, QGS/QPS, Cedars-Sinai Medical Center, Los Angeles, CA) was used to calculate left ventricular (LV) volumes and ejection fraction (EF) and the scores incorporating both the extent and severity of perfusion defects, using standardized segmentation of 17 myocardial regions (11). Briefly, this commercial package determines reconstruction limits for the projection dataset, reconstructs the projection images into transaxial images using standard filtered backprojection, and then reorients the transaxial images into short-axis images. LV contours were checked visually and manually adjusted if the computer-generated automatic contours were found to be incorrect. Quantitative defect extent and severity were defined from sex-specific normal limits, and summed stress score (SSS) was obtained by adding the scores of the 17 segments (0 = normal to 4 = absent perfusion) of the stress images. A similar procedure is applied to the resting images to calculate the summed rest score (SRS). The summed difference score (SDS) represents the difference between the stress and rest scores and is taken to be an index of ischemic burden. A post-stress LVEF >45% and a summed stress score <3 were considered normal (12). The total perfusion defect (TPD) of the stress and resting images was generated, representing the defect extent and severity and expressed as a percentage of the left ventricular myocardium (13).

Patients were categorized into 3 groups of stress TPD (normal <5%; mild-moderate from 5% to 15% and severe abnormality >15%) (14).

CZT Camera: D-SPECT

The CZT camera recordings were obtained immediately after each rest or stress Anger camera scans. The D-SPECT technology (DSPECT, Spectrum Dynamics, Caesarea, Israel) (15) uses 9 pixilated cadmium zinc telluride crystal detector columns mounted vertically spanning a 90° geometry. Each of the columns consists of 1,024 (16 x 64) 5-mm thick cadmium zinc telluride crystal elements (2.46 x 2.46 mm). Square-hole tungsten collimators are fitted to each of the detectors, which are shorter than conventional low-energy, high-resolution collimators, yielding significantly better geometric speed. Data are acquired focusing on the heart by the detectors rotating in synchrony and saved in list mode. The CZT camera uses a proprietary Broadview reconstruction algorithm based on the maximum likelihood expectation maximization algorithm (16–18). Images were acquired with the patient in a semi recumbent position. A 10-s pre-scan acquisition was performed to identify the location of the heart and to set the angle limits of scanning for each detector (region of interest– centric scanning). A 4-min rest acquisition (120 projections per detector, 2 s per projection) was performed after resting conventional SPECT imaging, and a 2-min acquisition (1 s per projection) followed the post-stress conventional SPECT imaging. Summed and gated projections were reconstructed with an iterative maximum likelihood expectation maximization algorithm using 7 and 4 iterations, respectively. An automated software program (QGS/QPS, Cedars-Sinai Medical Center, Los Angeles, CA) was used to calculate LV volumes, EF and the scores incorporating both the extent and severity of resting and post-stress perfusion defects, using standardized segmentation of 17 myocardial regions (SSS, SRS, SDS and TPD) (11).

Statistical analysis

Statistical analysis was performed with a commercially available software package (SPSS, version 20.0 for Windows, SPSS Inc., Chicago, IL, USA) and Statistics with R (version 3.4.0). Semi-quantitative variables were expressed as mean ± SD, and categorical variables as frequencies or percentage. Correlations between SSS, SRS, EDV, ESV, LVEF and TPD, by D-SPECT versus conventional SPECT were evaluated by linear regression, and differences between the two methods were assessed by Bland-Altman analysis (19). Concordance between the methods was assessed using kappa analysis. A p-value of less than 0.05 was considered as statistically significant. Comparison of continuous data between groups was performed using the two-sided Student's t test. In patients with angiographic available data, sensitivity, specificity, positive predictive value (PPV), negative predictive value (NPV) and diagnostic accuracy for the detection of CAD (≥50% luminal narrowing) were calculated for conventional SPECT and D-SPECT.

Results

Patient characteristics

Table 1 summarizes the clinical characteristics of the patient population. The study group comprised 287 (55%) with suspected and 230 (45%) with known CAD. In patients with suspected CAD, pre-scan likelihood of disease was low in 185 (64%) patients and intermediate to high in 102 (36%) patients. Of the overall 517 patients analyzed, 266 (51%) performed treadmill exercise stress test whereas 251 (49%) dipyridamole stress test.

Correlation of perfusion scores

The mean perfusion scores of conventional and D-SPECT are summarized in Table 2.

As shown in Figure 1A, an excellent linear correlation between SSS by conventional SPECT versus SSS by D-SPECT (r=0.808, p <0.001) has been demonstrated. In the Bland-Altman analysis,

(Figure 1B) the mean difference in SSS between conventional SPECT and D-SPECT was 1.3%. The lower and upper limits of agreement between the two techniques were −7.46% to 10%.

Similarly, SRS by D-SPECT excellently correlated to SRS by conventional SPECT (r= 0.915, p<0.001) (Figure 2A). The Bland-Altman analysis for the SRS between conventional SPECT and D-SPECT showed a mean difference of 0.55 % and (Figure 2B) and the lower and upper limits of agreement between the two techniques −4.85% to 6% (Figure 2B).

As well, semi-quantitative stress TPD by D-SPECT demonstrated linear correlation with conventional SPECT (r=0.892, p< 0.001) (Figure 3A). The Bland-Altman analysis for the TPD between conventional SPECT and D-SPECT showed a mean difference of 0.54 % and (Figure 3B) and the lower and upper limits of agreement between the two techniques −8.86% to 9.94% (Figure 3B).

Correlation of functional scores

The mean functional scores of conventional and D-SPECT are summarized in Table 2.

As shown in Figure 4A, an excellent linear correlation between EDV by conventional SPECT versus EDV by D-SPECT (r=0.911, p <0.001) has been demonstrated. In the Bland-Altman analysis, the mean difference in EDV between conventional SPECT and D-SPECT was -13% (Figure 4B). The lower and upper limits of agreement between the two techniques were −39.9% to 13.7% (Figure 4B).

Similarly, ESV by D-SPECT excellently correlated to ESV by conventional SPECT (r= 0.926, p<0.001) (Figure 5A). The Bland-Altman analysis for the ESV between conventional SPECT and D-SPECT showed a mean difference of -8% and (Figure 5B) and the lower and upper limits of agreement between the two techniques −17.7% to 17.7% (Figure 5B).

The correlation between LVEF by the methods was linear over a wide range of EF values (r =0.82, p<0.001) (Figure 6A).

The Bland-Altman analysis for the EF between conventional SPECT and D-SPECT showed a mean difference of 3.4% and (Figure 6B) and the lower and upper limits of agreement between the two techniques −15.6% to 22.4% (Figure 6B).

Concordance of Stress Perfusion Findings

Patients were analyzed into 3 groups of stress TPD (normal <5%; mild-moderate from 5% to 15%; and severe abnormality> 15%). By conventional SPECT, 198 patients had normal MPI and 319 had abnormal MPI, 252 mild or moderate and 67 severe defects. By D-SPECT, 254 patients had normal MPI and 263 abnormal MPI, 188 mild or moderate and 75 severe perfusion deficits. The concordance between the methods has showed in Table 3.

In patients with normal findings by conventional SPECT, the mean SSS, SRS and TPD were 2.61±2, 0.22±0.6 and 2.31±1, respectively. The mean EDV, ESV and EF were 78.88±23, 32.09±17 and 61.72±12 respectively. In patients with mild or moderate defects, the mean SSS, SRS and TPD were 7.29±3, 2.23±3 and 8.36±3, respectively. The mean EDV, ESV and EF were 70.19±28, 28.86±22 and 64.3±17 respectively. In patients with severe defects, the mean SSS, SRS and TPD were 21.36±8, 17.33±9 and 30.22±11, respectively. The mean EDV, ESV and EF were 121.85±55, 75.37±46 and 41.37±14 respectively.

In patients with normal findings by D-SPECT, the mean SSS, SRS and TPD were 1.39±1, 0.7±0.4 and 2.08±1.2, respectively. The mean EDV, ESV and EF were 79.51±27, 32.46±19 and 61.61±10 respectively. In patients with mild or moderate defects, the mean SSS, SRS and TPD were 6.47±3, 1.86±2 and 8.41±3, respectively. The mean EDV, ESV and EF were 92.98±29, 42.02±20 and 56.85±10 respectively. In patients with severe defects, the mean SSS, SRS and TPD were 20.07±8, 14.84±8 and 29.33±12, respectively. The mean EDV, ESV and EF were 147.28±60, 94.34±54 and 39.34±12 respectively.

Diagnostic performance of conventional SPECT compared to D-SPECT

Diagnostic performance of conventional and CZT SPECT is showed in Figure 7. In 86 patients with coronary angiography data available, conventional SPECT yields sensitivity and specificity of 95% and 75% respectively, while for D-SPECT sensitivity and specificity of 86% and 85% were recorded. No statistical differences in sensitivity and specificity have been observed between the two methods (p=0.12 and p=0.36, respectively). Moreover, the diagnostic accuracy for conventional SPECT and D-SPECT was not different (88% and 84%, respectively, p=0.5). As well, the PPV and NPV for conventional and D-SPECT were 88% and 84%, p=0.48 and 87% and 85%, p=0.8, respectively.

Discussion

Coronary artery disease (CAD) remains one of the leading cause of mortality in the developed countries, however epidemiologic data show that improved control of cardiac risk factors has resulted in a temporal decrement in the incidence and severity of CAD as well as its related mortality. (20) Stress single-photon emission computed tomography myocardial perfusion imaging (MPI) is a well-established modality for the evaluation and analysis of global and regional left ventricular function in patients with suspected or known CAD. This technique has clinical advantages including high sensitivity and high negative predictive value (NPV) (21).

Stress myocardial SPECT imaging has been markedly enhanced by the recent commercialization of cameras with semiconductor with cadmium-zinc-telluride (CZT) detectors (22). These new cameras offer higher energy resolution and higher count sensitivity, thereby allowing improved image quality overcoming the considerable limitations of the conventional gamma camera as the prolonged time to scan acquisition and the radiation dose (23). CZT cameras use a different imaging technique compared to conventional SPECT cameras, with a stationary multi-pinhole design focused on the heart. This new geometric design and the new detector material combined with novel reconstruction algorithms led to improved diagnostic performance. Since the introduction of the novel dedicated cardiac CZT camera in 2006, several clinical studies confirmed the high performance of this new camera (24). These studies evaluated its physical characteristics and the overall performances in comparison to conventional Anger cameras, and tested the potential to reduce scan times and/or tracer activity and their effectiveness in clinical use (4, 14, 21, 22). The superior performances reported for CZT system in comparison to conventional Anger cameras, are strictly dependent on the intrinsically different technology and acquisition techniques, which are, in clinical conditions, potentially capable of producing significantly different results (25).

Quantitative analysis has been shown to be useful in comparing sequential MPI studies (26, 27) and assessing the effectiveness of invasive as well as medical treatments in patients with CAD (28) and to provide evidence of the generalizability of the SPECT MPI results with the new system.

Sharir et al. (14) have compared the conventional gamma camera systems and new high-speed technology, demonstrating that high-speed stress and rest TPD correlated linearly with conventional SPECT TPD ($r = 0.95$ and 0.97, respectively, $p < 0.0001$), with good concordance in the 3 vascular territories (k for the left anterior descending coronary artery, left circumflex coronary artery, and right coronary artery were 0.73, 0.73, and 0.70, respectively; >90% agreement).

Moreover, a recent multicenter study evaluating a new solid-state cardiac camera showed diagnostic performance comparable to that of standard SPECT cameras, with superior image quality and significantly shorter acquisition time (7). In the present investigation, D-SPECT performance was compared with conventional SPECT in detecting perfusion abnormalities by stress-only Tc-99m sestamibi protocol, in 517 patients referred for evaluation of CAD at our institution. The results of our study highlight excellent correlation between D-SPECT and traditional camera in the evaluation of perfusion scores (SSS, SRS, TPD) and parameters of left ventricular function (EDV, ESV, LVEF). However, comparing mean values of SSS, SRS, TPD, EDV, ESV and EF some differences were found between conventional SPECT and D-SPECT.

The diagnostic accuracy evaluated in the 86 patients with coronary angiography available data, was not significantly different between conventional camera and D-SPECT but showed a trend to a higher specificity (75% compared to 85% by traditional camera). These findings may be explained by the functioning of novel CZT cameras: patient position (upright or supine) and the position of the detectors closer to patients body reduce attenuation artifacts, limiting the overestimation of the perfusion defect scores obtained by conventional SPECT; similarly higher patient comfort and short-time acquisition of D-SPECT decrease motion artifacts. Moreover, our results showed that D-SPECT has more normal scans, as already demonstrated by Lima et al. (6), with a modest agreement and concordance between both cameras, when patients were categorized on the basis of TPD (agreement 61%, k=0.37).

Conclusion

The novel CZT camera provides excellent image quality, which is equivalent to standard myocardial SPECT, despite a short scan time of less than half the standard time.

Quantitative measures of myocardial perfusion and function, obtained using normal limits specific for the new technology, correlated extremely well with respective conventional SPECT measures.

These findings support the use of this technology in nuclear laboratories using various radiopharmaceutical and stress protocols, evaluating patient populations with suspected or known CAD.

References

1. Anger HO. Scintillation camera with multichannel collimators. J Nucl Med 1964 Jul; 5:515–31.
2. Sharir T, Ben-Haim S, Merzon K, Prochorov V, Dickman D, Ben-Haim S, Berman DS. High-speed myocardial perfusion imaging initial clinical comparison with conventional dual detector anger camera imaging. JACC Cardiovasc Imaging 2008 Mar; 1:156–63.
3. Berman DS, Kang X, Tamarappoo B, Wolak A, Hayes SW, Nakazato R, et al. Stress thallium-201/rest technetium-99 m sequential dual isotope high-speed myocardial perfusion imaging. JACC Cardiovasc Imaging 2009 Mar; 2: 273–282.
4. Esteves FP, Raggi P, Folks RD, Keidar Z, Askew JW, Rispler S, et al. Novel solid-state-detector dedicated cardiac camera for fast myocardial perfusion imaging: Multicenter comparison with standard dual detector cameras. J Nucl Cardiol 2009 Nov-Dec; 16: 927–934.
5. Slomka PJ, Patton JA, Berman DS, Germano G. Advances in technical aspects of myocardial perfusion SPECT imaging. J Nucl Cardiol 2009 Mar-Apr; 16: 255–276.
6. Lima R, Peclat T, Soares T, Ferreira C, Souza AC, Camargo G. Comparison of the prognostic value of myocardial perfusion imaging using a CZT-SPECT camera with a conventional anger camera. J Nucl Cardiol 2017 Feb; 24:245–251.
7. Tanaka H, Chikamori T, Hida S, Uchida K, Igarashi Y, Yokoyama T, Takahashi M, Shiba C, Yoshimura M, Tokuuye K, Yamashina A. Comparison of myocardial perfusion imaging between the new high-speed gamma camera and the standard anger camera. Circ J 2013; 77:1009–17.
8. Diamond GA, Staniloff HM, Forrester JS, et al. Computer assisted diagnosis in the noninvasive evaluation of patients with suspected coronary artery disease. J Am Coll Cardiol 1983 Feb; 1:444–55.

9. Hesse B, Tägil K, Cuocolo A, Anagnostopoulos C, Bardiés M, Bax J, et al. EANM/ESC procedural guidelines for myocardial perfusion imaging in nuclear cardiology. Eur J Nucl Med Mol Imaging 2005 Jul; 32:855–97.
10. Acampa W, Petretta M, Evangelista L, Daniele S, Xhoxhi E, De Rimini ML, et al. Myocardial perfusion imaging and risk classification for coronary heart disease in diabetic patients. The IDIS study: A prospective, multicentre trial. Eur J Nucl Med Mol Imaging 2012 Mar; 39:387–95.
11. Germano G, Kavanagh PB, Waechter P, Areeda J, Van Kriekinge S, Sharir T, et al. A new algorithm for the quantitation of myocardial perfusion SPECT. I: Technical principles and reproducibility. J Nucl Med 2000 Apr; 41:712–9.
12. Acampa W, Petretta M, Daniele S, Del Prete G, Assante R, Zampella E, et al. Incremental prognostic value of stress myocardial perfusion imaging in asymptomatic diabetic patients. Atherosclerosis 2013 Apr; 227:307–12.
13. Slomka PJ, Nishina H, Berman DS, Kang X, Friedman JD, et al. Automatic quantification of myocardial perfusion stress-rest change: a new measure of ischemia. J Nucl Med 2004 Feb; 45:183–91.
14. Sharir T, Slomka PJ, Hayes SW, DiCarli MF, Ziffer JA, Martin WH, Dickman D, Ben-Haim S, Berman DS. Multicenter trial of high-speed versus conventional single-photon emission computed tomography imaging: quantitative results of myocardial perfusion and left ventricular function. J Am Coll Cardiol 2010 May; 55:1965–74.
15. Gambhir SS, Berman DS, Ziffer J, et al. A novel high sensitivity rapid acquisition single photon cardiac imaging camera. J Nucl Med 2009 Apr; 50:635–43.
16. Shepp LA, Vardi Y. Maximum likelihood reconstruction for emission tomography. IEEE Trans Med Imaging 1982; 1:113–22.
17. Lange K, Carson R. EM reconstruction algorithms for emission and transmission tomography. J Comput Assist Tomogr 1984 Apr; 8:306–16.

18. Hudson HM, Larkin RS. Accelerated image reconstruction using ordered subsets of projection data. IEEE Trans Med Imaging 1994; 13:601–9.

19. Bland JM, Altman D. Statistical methods for assessing agreement between two methods of clinical measurement. Lancet 1986 Feb; 1:307–10.

20. Go AS, Mozaffarian D, Roger VL, Benjamin EJ, Berry JD, Blaha MJ, et al. American Heart Association Statistics Committee and Stroke Statistics Subcommittee. Heart disease and stroke statistics--2014 update: a report from the American Heart Association. Circulation 2014 Jan; 129:e28–e292.

21. Duvall WL, Rai M, Ahlberg AW, O'Sullivan DM, Henzlova MJ. A multi-center assessment of the temporal trends in myocardial perfusion imaging. J Nucl Cardiol 2015 Jun; 22:539–51.

22. Imbert L, Poussier S, Franken PR, Songy B, Verger A, Morel O, Wolf D, Noel A, Karcher G, Marie PY. Compared performance of high-sensitivity cameras dedicated to myocardial perfusion SPECT: a comprehensive analysis of phantom and human images. J Nucl Med 2012 Dec; 53:1897–903.

23. Verger A, Djaballah W, Fourquet N, Rouzet F, et al. Comparison between stress myocardial perfusion SPECT recorded with cadmium-zinc-telluride and Anger cameras in various study protocols. Eur J Nucl Med Mol Imaging 2013 Feb; 40:331–40.

24. Mouden M, Timmer JR, Ottervanger JP, Reiffers S, Oostdijk AH, et al. Impact of a new ultrafast CZT SPECT camera for myocardial perfusion imaging: fewer equivocal results and lower radiation dose. Eur J Nucl Med Mol Imaging 2012 Jun; 39:1048–55.

25. Zoccarato O, Lizio D, Savi A, Indovina L, Scabbio C, Leva L, Del Sole A, Marcassa C, et al. Comparative analysis of cadmium-zincum-telluride cameras dedicated to myocardial perfusion SPECT: A phantom study. J Nucl Cardiol 2016 Aug; 23:885–93.

26. Slomka PJ, Berman DS, Germano G. Quantification of serial changes in myocardial perfusion. J Nucl Med 2004 Dec; 45:1978–80.

27. Berman DS, Kang X, Gransar H, et al. Quantitative assessment of myocardial perfusion abnormality on SPECT myocardial perfusion imaging is more reproducible than expert visual analysis. J Nucl Cardiol 2009 Jan-Feb; 16:45–53.
28. Shaw LJ, Berman DS, Maron DJ, et al. Optimal medical therapy with or without percutaneous coronary intervention to reduce ischemic burden: results from the Clinical Outcomes Utilizing Revascularization and Aggressive Drug Evaluation (COURAGE) trial nuclear substudy. Circulation 2008 Mar; 117:1283–91.

Table 1. Clinical characteristics of patients

	n = 517
Age (years)	63 ± 10
Male gender	377 (73)
Diabetes	177 (34)
Dyslipidemia	377 (73)
Smoking	232 (45)
Hypertension	447 (86)
Angina-like symptom	186 (36)
Family history of CAD	255 (49)
Previous MI	174 (34)
Previous revascularization procedures	197 (38)
BMI ≥ 30	126 (24)

Data are presented as mean ±SD or n (%).

CAD, coronary artery disease; *MI*, myocardial infarction; *BMI*, body mass index.

Table 2. Conventional and D-SPECT perfusion and functional scores

	N	Conventional SPECT	D-SPECT	p-value
SSS	517	7.32±7	5.95±7	.000
SRS	250	3.41±7	2.86±6	.000
SDS	250	2.97±3	4.16±3	.000
TPD	517	8.88±10	8.34±10	.010
EDV	472	80.16±35	93.3±40	.000
ESV	472	36±28	44.1±33	.000
EF	472	60.39±16	56.9±12	.000

Data are presented as mean ±SD.

SSS, summed stress score; *SRS*, summed rest score;

SDS, summed difference score; *TPD*, total perfusion deficit;

EDV, end-diastolic volume; *ESV*, end-systolic volume; *EF*, ejection fraction.

Table 3. Concordance of perfusion score findings

	D-SPECT			
Conventional SPECT	Normal	Mild-moderate perfusion defect	Severe perfusion defect	Total
Normal	138	59	1	198
Mild-moderate perfusion defect	116	121	15	252
Severe perfusion defect	0	8	59	67
Total	254	188	75	517

Agreement 61%, kappa = 0.37

SPECT, single-photon emission computed tomography

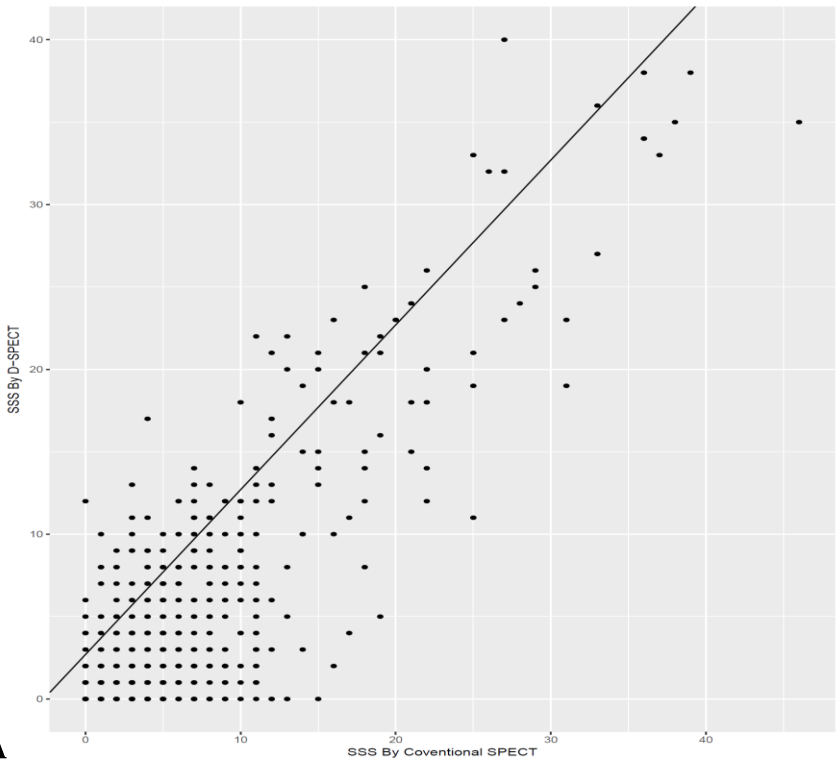

A

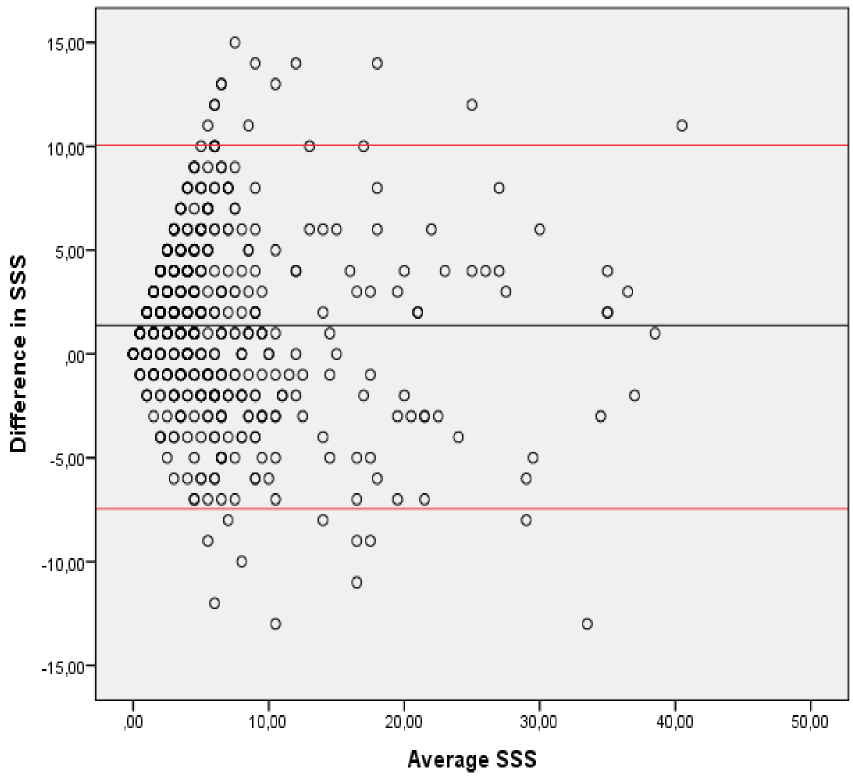

B

Figure 1. (A) Correlation of Quantitative SSS by D-SPECT versus conventional SPECT. **(B)** Bland-Altman plot for SSS by D-SPECT versus conventional SPECT.

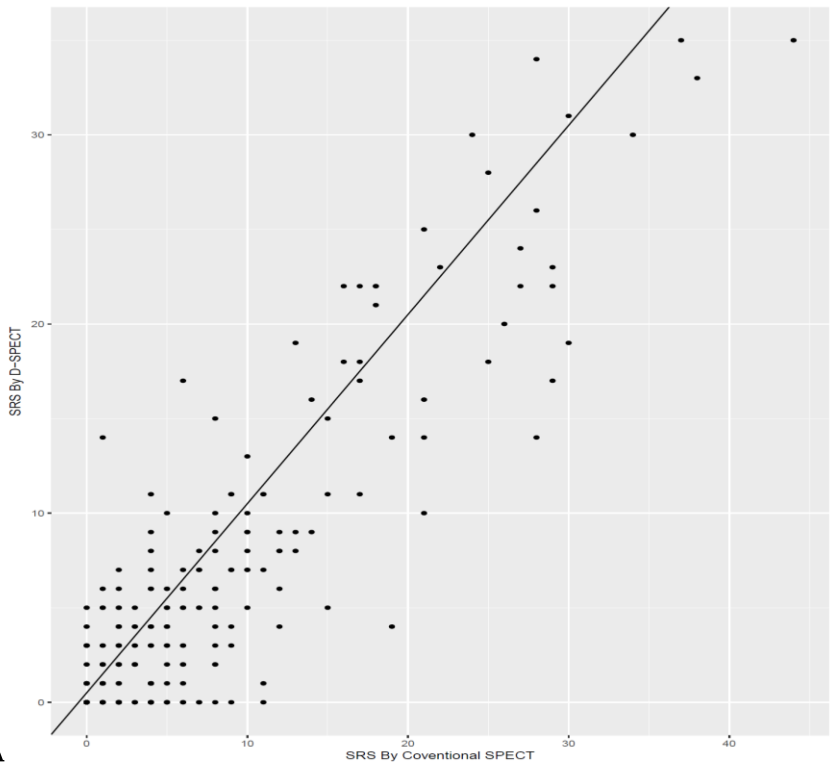

A

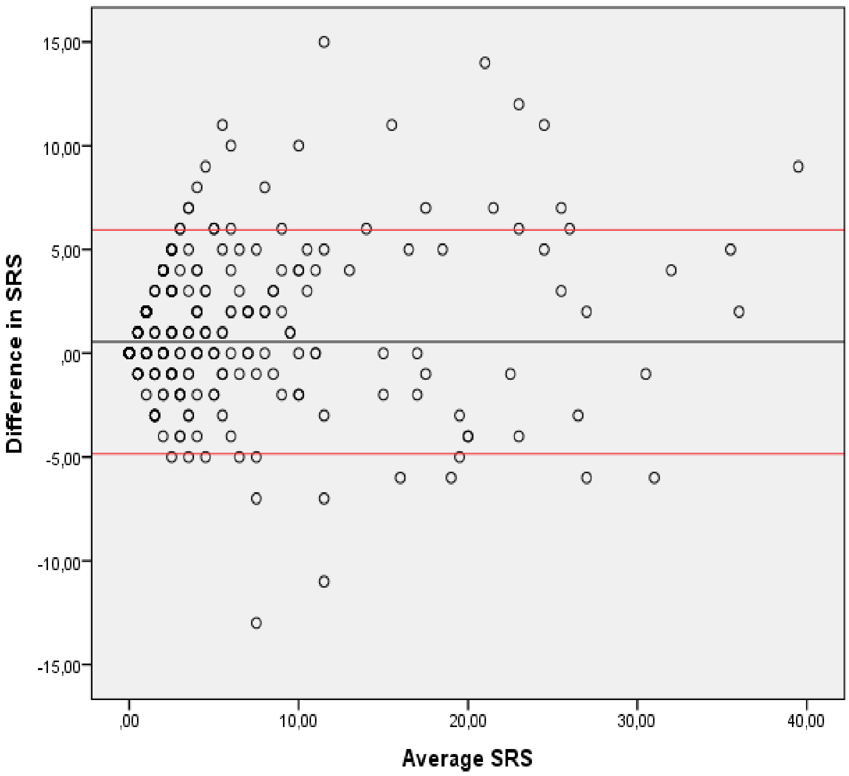

B

Figure 2. (A) Correlation of Quantitative SRS by D-SPECT versus conventional SPECT. **(B)** Bland-Altman plot for SRS by D-SPECT versus conventional SPEC

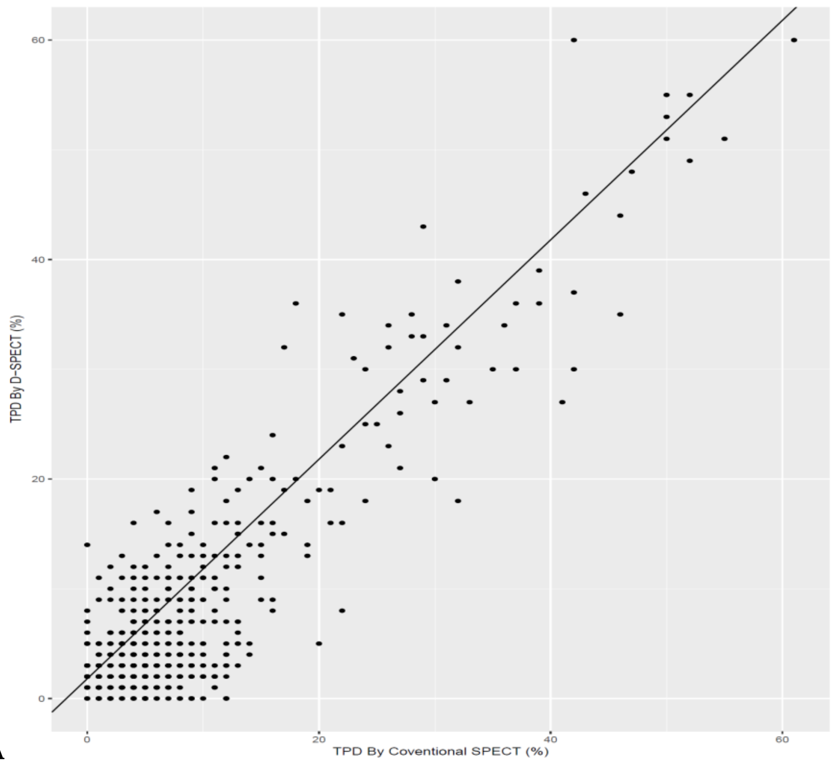

A

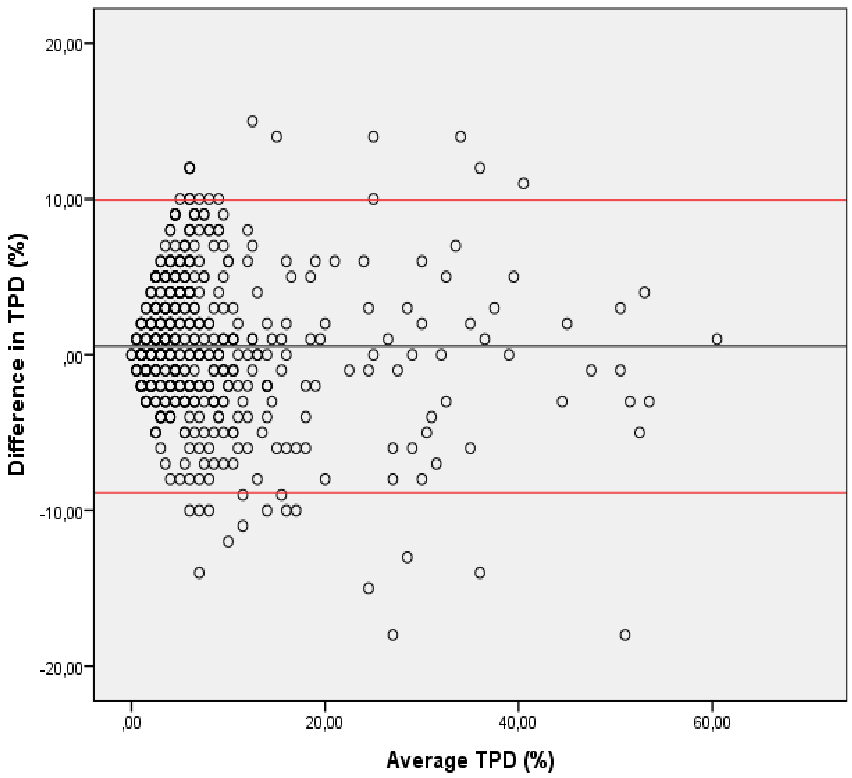

B

Figure 3. (A) Correlation of TPD (%) by D-SPECT versus conventional SPECT. **(B)** Bland-Altman plot for TPD (%) by D-SPECT versus conventional SPECT

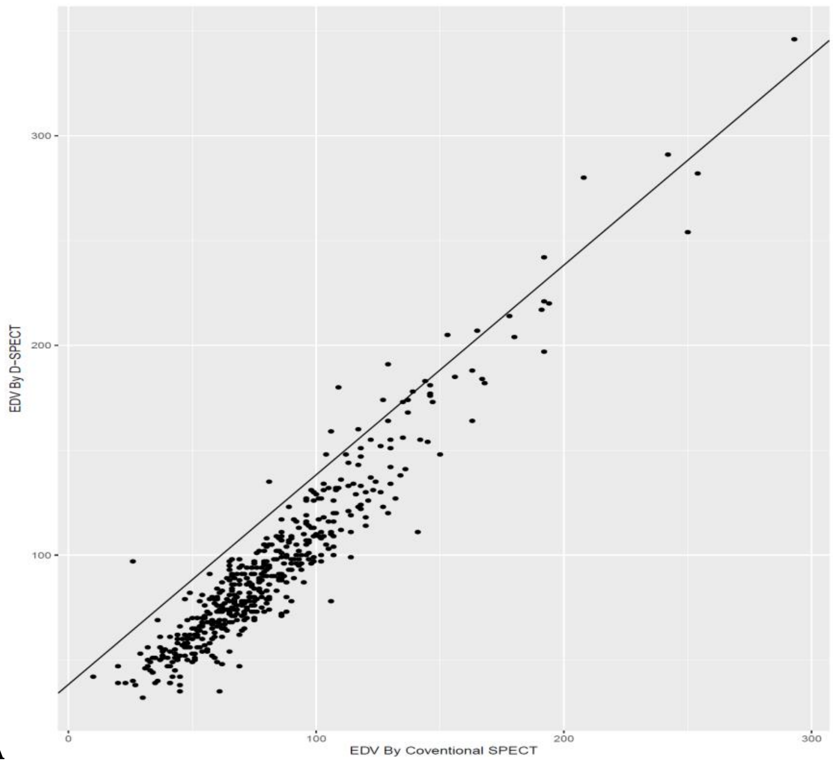

A

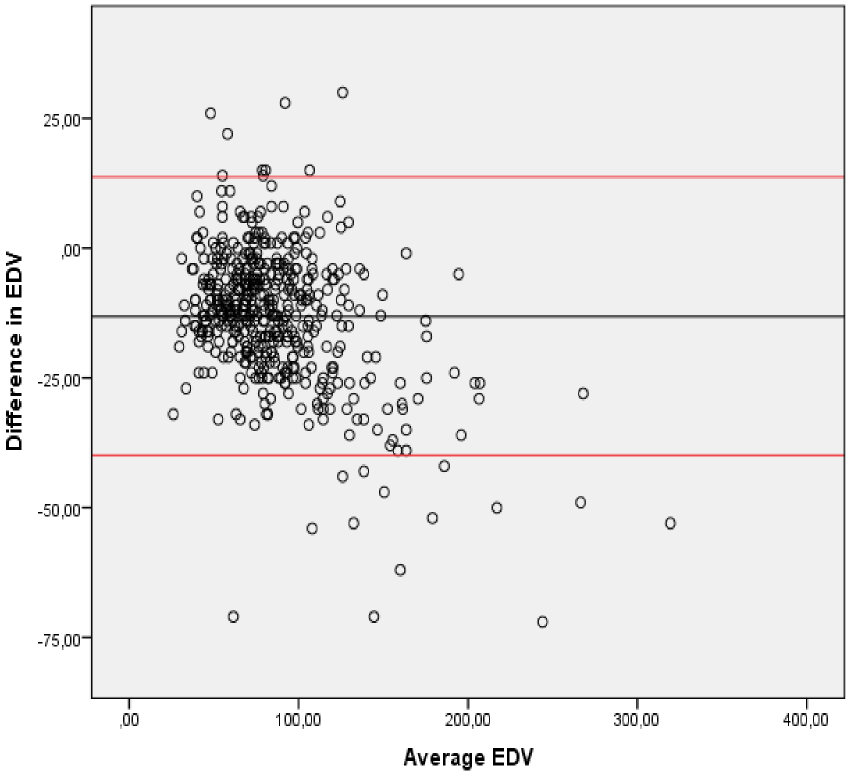

B

Figure 4. (A) Correlation of EDV by D-SPECT versus conventional SPECT. **(B)** Bland-Altman plot for EDV by D-SPECT versus conventional SPECT

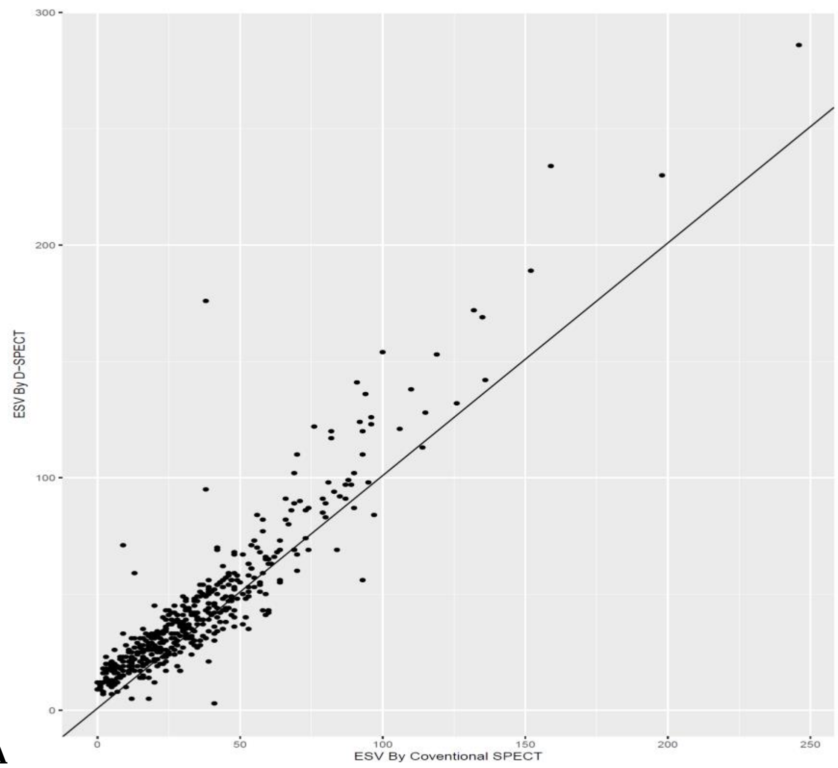

A

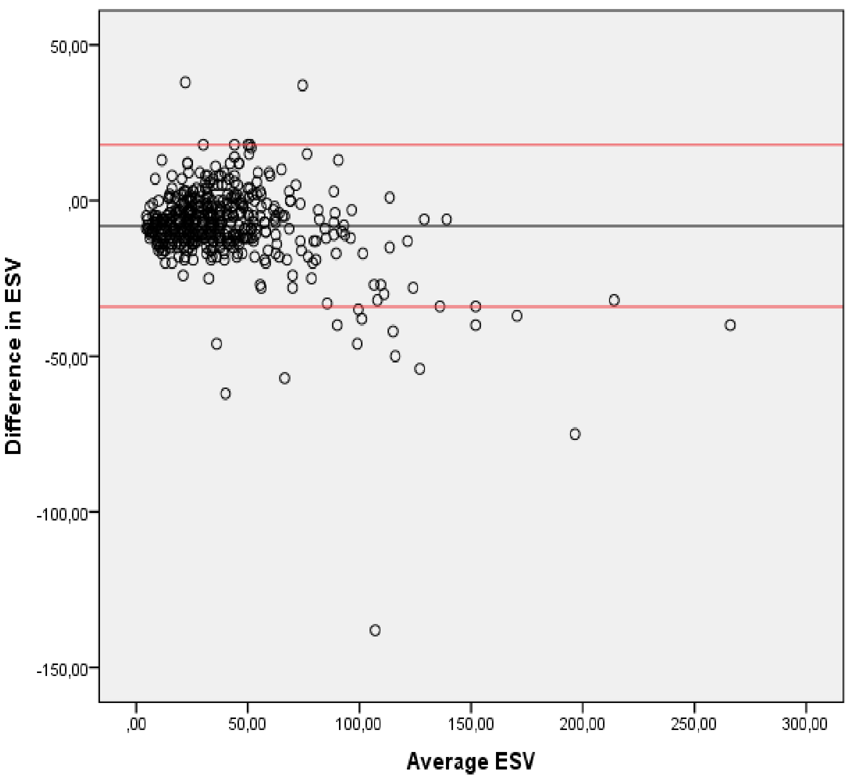

B

Figure 5. (A) Correlation of ESV by D-SPECT versus conventional SPECT. **(B)** Bland-Altman plot for ESV by D-SPECT versus conventional SPECT.

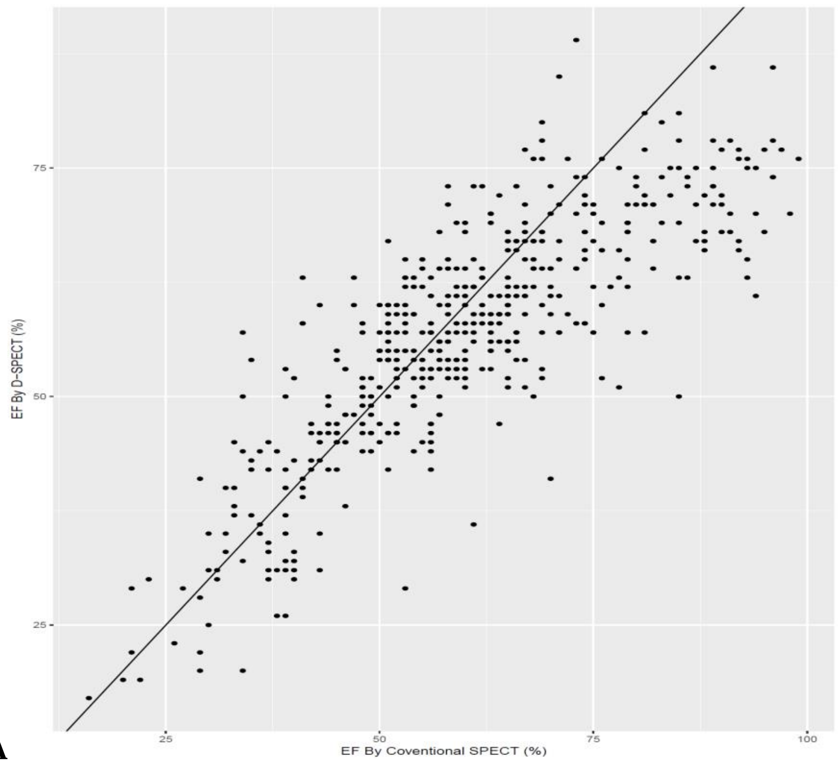

A

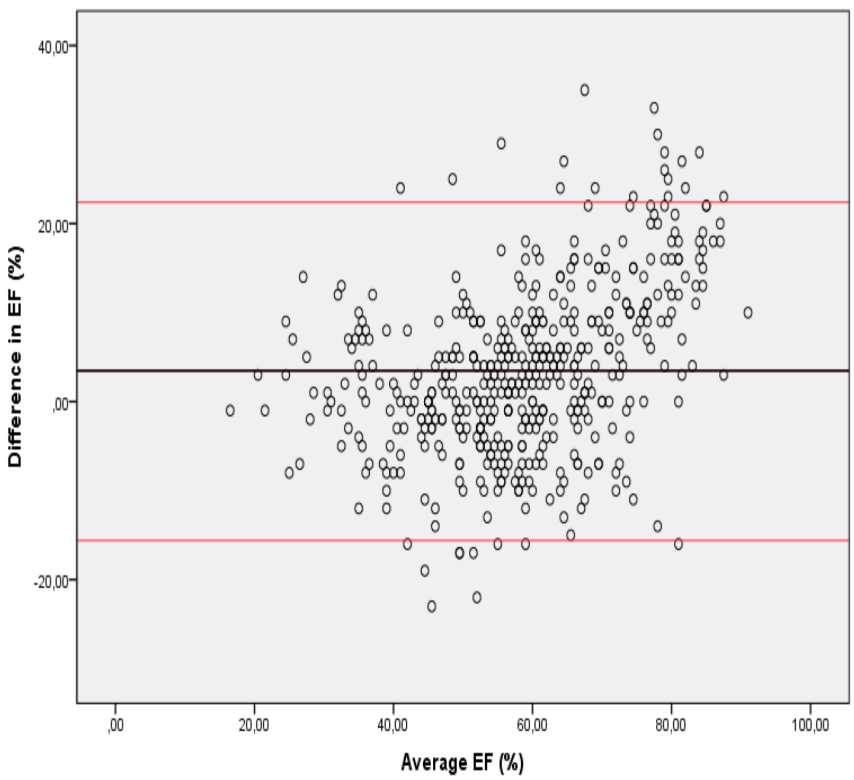

B

Figure 6. (A) Correlation of EF by D-SPECT versus conventional SPECT. **(B)** Bland-Altman plot for EF by D-SPECT versus conventional SPECT.

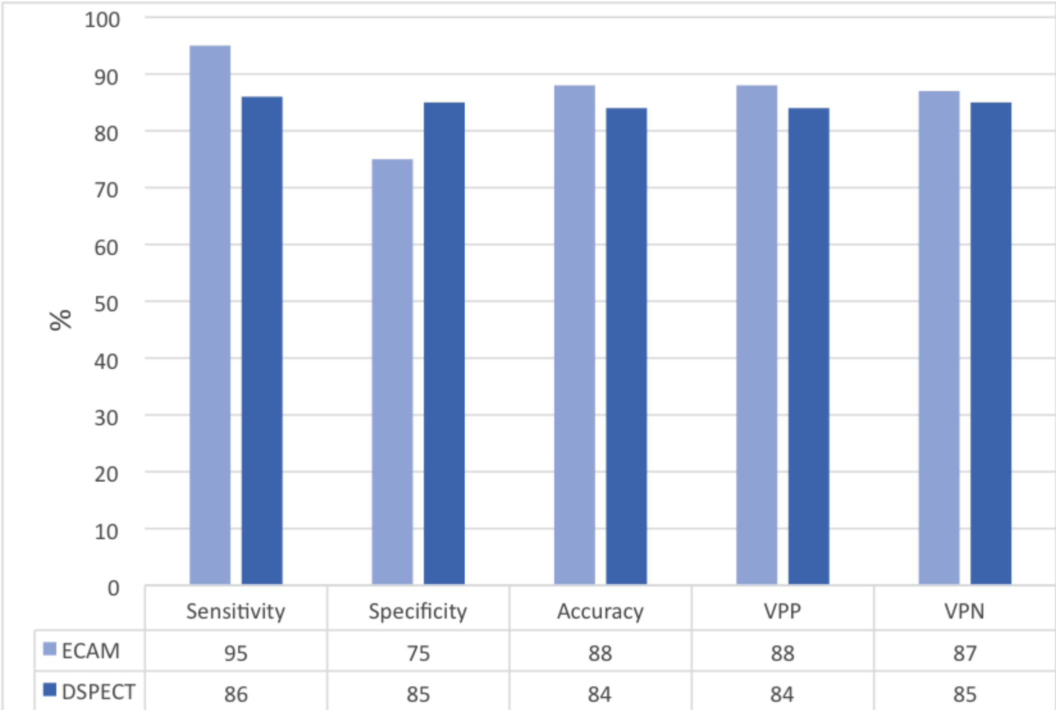

Figure 7. Diagnostic performance of conventional SPECT compared to D-SPECT

References

1. Anger HO. Scintillation camera with multichannel collimators. J Nucl Med 1964;5:515–31.
2. Sharir T, Ben-Haim S, Merzon K, Prochorov V, Dickman D, Ben-Haim S, Berman DS. High-speed myocardial perfusion imaging initial clinical comparison with conventional dual detector anger camera imaging. JACC Cardiovasc Imaging. 2008; 1(2):156-63.
3. Berman DS, Kang X, Tamarappoo B, Wolak A, Hayes SW, Nakazato R, et al. Stress thallium-201/rest technetium-99 m sequential dual isotope high-speed myocardial perfusion imaging. *JACC* Cardiovasc Imaging 2009; 2: 273 – 282.
4. Esteves FP, Raggi P, Folks RD, Keidar Z, Askew JW, Rispler S, et al. Novel solid-state-detector dedicated cardiac camera for fast myocardial perfusion imaging: Multicenter comparison with standard dual detector cameras. J Nucl Cardiol 2009; 16: 927 – 934.
5. Slomka PJ, Patton JA, Berman DS, Germano G. Advances in technical aspects of myocardial perfusion SPECT imaging. J Nucl Cardiol 2009; 16: 255 – 276.
6. Lima R, Peclat T, Soares T, Ferreira C, Souza AC, Camargo G. Comparison of the prognostic value of myocardial perfusion imaging using a CZT-SPECT camera with a conventional anger camera. J Nucl Cardiol. 2017; 24(1):245-251.
7. Tanaka H, Chikamori T, Hida S, Uchida K, Igarashi Y, Yokoyama T, Takahashi M, Shiba C, Yoshimura M, Tokuuye K, Yamashina A. Comparison of myocardial perfusion imaging between the new high-speed gamma camera and the standard anger camera. Circ J. 2013; 77(4):1009-17.
8. Diamond GA, Staniloff HM, Forrester JS, et al. Computer assisted diagnosis in the noninvasive evaluation of patients with suspected coronary artery disease. J Am Coll Cardiol 1983; 1:444 –5.

9. Hesse B, Tägil K, Cuocolo A, Anagnostopoulos C, Bardiés M, Bax J, et al. EANM/ESC procedural guidelines for myocardial perfusion imaging in nuclear cardiology. Eur J Nucl Med Mol Imaging 2005; 32:855-97.

10. Acampa W, Petretta M, Evangelista L, Daniele S, Xhoxhi E, De Rimini ML, et al. Myocardial perfusion imaging and risk classification for coronary heart disease in diabetic patients. The IDIS study: A prospective, multicentre trial. Eur J Nucl Med Mol Imaging 2012; 39:387-95.

11. Germano G, Kavanagh PB, Waechter P, Areeda J, Van Kriekinge S, Sharir T, et al. A new algorithm for the quantitation of myocardial perfusion SPECT. I: Technical principles and reproducibility. J Nucl Med 2000; 41:712-9.

12. Acampa W, Petretta M, Daniele S, Del Prete G, Assante R, Zampella E, et al. Incremental prognostic value of stress myocardial perfusion imaging in asymptomatic diabetic patients. Atherosclerosis 2013; 227:307-12.

13. Slomka PJ, Nishina H, Berman DS, Kang X, Friedman JD, et al. Automatic quantification of myocardial perfusion stress-rest change: a new measure of ischemia. J Nucl Med. 2004; 45(2):183-91.

14. Sharir T, Slomka PJ, Hayes SW, DiCarli MF, Ziffer JA, Martin WH, Dickman D, Ben-Haim S, Berman DS. Multicenter trial of high-speed versus conventional single-photon emission computed tomography imaging: quantitative results of myocardial perfusion and left ventricular function. J Am Coll Cardiol. 2010; 55(18):1965-74.

15. Gambhir SS, Berman DS, Ziffer J, et al. A novel high sensitivity rapid acquisition single photon cardiac imaging camera. J Nucl Med 2009; 50:635– 43.

16. Shepp LA, Vardi Y. Maximum likelihood reconstruction for emission tomography. IEEE Trans Med Imaging 1982; 1:113–22.

17. Lange K, Carson R. EM reconstruction algorithms for emission and transmission tomography. J Comput Assist Tomogr 1984; 8:306 –16.
18. Hudson HM, Larkin RS. Accelerated image reconstruction using ordered subsets of projection data. IEEE Trans Med Imaging 1994; 13:601–9.
19. Bland JM, Altman D. Statistical methods for assessing agreement between two methods of clinical measurement. Lancet 1986; 1:307–10.
20. Go AS, Mozaffarian D, Roger VL, Benjamin EJ, Berry JD, Blaha MJ, et al. American Heart Association Statistics Committee and Stroke Statistics Subcommittee. Heart disease and stroke statistics--2014 update: a report from the American Heart Association. Circulation. 2014 Jan 21; 129(3):e28-e292.
21. Duvall WL, Rai M, Ahlberg AW, O'Sullivan DM, Henzlova MJ. A multi-center assessment of the temporal trends in myocardial perfusion imaging. J Nucl Cardiol. 2015; 22(3):539-51.
22. Imbert L, Poussier S, Franken PR, Songy B, Verger A, Morel O, Wolf D, Noel A, Karcher G, Marie PY. Compared performance of high-sensitivity cameras dedicated to myocardial perfusion SPECT: a comprehensive analysis of phantom and human images. J Nucl Med. 2012; 53(12):1897-903.
23. Verger A, Djaballah W, Fourquet N, Rouzet F, et al. Comparison between stress myocardial perfusion SPECT recorded with cadmium-zinc-telluride and Anger cameras in various study protocols. Eur J Nucl Med Mol Imaging. 2013; 40(3):331-40.
24. Mouden M, Timmer JR, Ottervanger JP, Reiffers S, Oostdijk AH, et al. Impact of a new ultrafast CZT SPECT camera for myocardial perfusion imaging: fewer equivocal results and lower radiation dose. Eur J Nucl Med Mol Imaging. 2012; 39(6):1048-55.
25. Zoccarato O, Lizio D, Savi A, Indovina L, Scabbio C, Leva L, Del Sole A, Marcassa C, et al. Comparative analysis of cadmium-zincum-telluride cameras dedicated to myocardial perfusion SPECT: A phantom study. J Nucl Cardiol. 2016; 23(4):885-93.

26. Slomka PJ, Berman DS, Germano G. Quantification of serial changes in myocardial perfusion. J Nucl Med 2004; 45:1978–80

27. Berman DS, Kang X, Gransar H, et al. Quantitative assessment of myocardial perfusion abnormality on SPECT myocardial perfusion imaging is more reproducible than expert visual analysis. J Nucl Cardiol 2009; 16:45–53.

28. Shaw LJ, Berman DS, Maron DJ, et al. Optimal medical therapy with or without percutaneous coronary intervention to reduce ischemic burden: results from the Clinical Outcomes Utilizing Revascularization and Aggressive Drug Evaluation (COURAGE) trial nuclear substudy. Circulation 2008;117:1283–91